

Relationship between Dispersion and Conductivity of Polymer Nanocomposites: A Molecular Dynamics Study

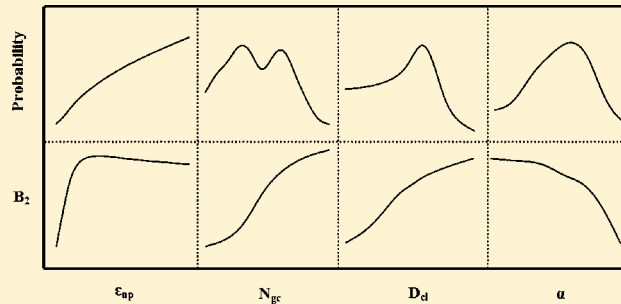
Yancong Feng,^{†,‡} Hua Zou,^{†,‡} Ming Tian,^{*,†,‡} Liqun Zhang,^{†,‡} and Jianguo Mi^{*,†,§}

[†]State Key Lab of Organic-Inorganic Composites, Beijing 100029, P. R. China

[‡]Center of Advanced Elastomer Materials, College of Materials Science and Engineering, Beijing University of Chemical Technology, Beijing 100029, P. R. China

[§]College of Chemical Engineering, Beijing University of Chemical Technology, Beijing 100029, P. R. China

ABSTRACT: The dispersive and conductive properties of polymer nanocomposites are investigated simultaneously using the molecular dynamics simulation method. Four factors influencing the dispersion and conductivity are concerned, including polymer–nanoparticle interaction, nanoparticles with grafted chains, cross-linking of polymer chains, and blending of polymer. It is shown that the variation of the conductive probability is not linearly related to the corresponding dispersion for all the four concerned cases. As the interaction strength increases, the dispersion of the nanoparticles appears to first increase and then drop, while the conductive probability increases monotonously. Increase of the grafting density on nanoparticles can bring about the modification of the dispersion, whereas the variation of the conductive probability is M-type. The dispersion effect increases monotonously with the increasing cross-linking density, but the corresponding conductive probability appears to first increase and then drop. The dispersive effect of nanoparticles monotonously decreases as the ratio of added incompatible polymer increases; however, the corresponding conductive probability has the maximum value.



1. INTRODUCTION

It is well-known that nonconductive polymer matrix filled with conductive nanoparticles can dramatically improve its electrical properties. If the volume fraction of the nanoparticles reaches a critical value, a continuous path of touching or nearly touching forms in the polymer matrix, leading to a transition from nonconductivity to conductivity. Previous researches showed that the conductive behavior is related to the spatial distribution of fillers in the polymer.¹ If the dispersion is poor, it is necessary to add high content of fillers for a good conductivity, which may decrease the mechanical properties of the polymer nanocomposite. It is therefore important to reinforce the dispersion of fillers in polymer matrix. On the other hand, an overdispersion of the fillers may be unfavorable to achieve a high conductivity.^{2–4} In this regard, understanding the relationship between the dispersion and the conductivity is essential to develop high electrical conductive polymer composites with low nanoparticle content.

The characteristic of nanoparticles is an important factor to influence the conductive properties of polymer composites. Recently, conductive polymer nanocomposites have been extensively investigated by experiments.^{5–9} In these experiments, carbon nanotube and graphite as the fillers are the research emphases to enhance the conductive probability due to their special construction. So far, the dispersion of fillers remains a big challenge. The three main methods to improve the dispersion are solution compounding,^{10–12} in-situ polymer-

ization,^{13–15} and melt blending.^{16–18} These methods are noncovalent assemblies where the polymer matrix and the nanoparticles interact via relatively weak dispersive forces. Dispersion with solution compounding or in-situ polymerization is better than that with melt blending.^{19,20} However, the experimental approach cannot analyze the dispersion of fillers and explain the mechanism of conductive percolation on the microscopic scale.

Simulation provides another good choice to study the conductive behavior. Previous simulations of conductive properties focused on the shape of fillers. For example, Ma et al. used a three-dimensional Monte Carlo model to predict electrical conductivity of polymer composites filled with conductive arm-shaped fibers.²¹ The results showed that the conductivity decreases and the percolation threshold increases as the fiber aspect ratio decreases and the fibers become more curved. Oskouyi et al. investigated the effect of the aspect ratio of the nanoparticles and the tunneling distance on the percolation threshold by employing a three-dimensional continuous Monte Carlo algorithm.²² Rahatekar et al. used the dissipative particle dynamics method to simulate the mixtures of fiber and sphere. They found that gradually replacing fibers with an equal volume of spheres can increase

Received: June 13, 2012

Revised: October 10, 2012

Published: October 11, 2012



the percolation threshold, and replacing a small fraction of high aspect ratio fibers with short fibers leads to a reduction of percolation threshold.²³ Li et al. applied the Monte Carlo method to investigate the influence of nanotube waviness on the electrical properties of carbon nanotube-based composites.²⁴ The results revealed that the electrical conductivities of composites with straight nanotubes are higher than that of composites with wavy nanotubes, and the critical exponent of the power-law dependence of electrical conductivity on nanotube concentration increases with decreasing nanotube curl ratio. Zeng et al. adopted the Monte Carlo method to research the electrical percolation with nanotubes as fillers, and the results agree well with experimental data.²⁵ They found that a higher degree of the waviness or of anisotropy in the orientation of nanotubes contributes to the increase of the percolation threshold. However, these simulations focus only on the fillers, whereas the roles of polymer matrix were entirely disregarded.

In polymer nanocomposites, the dispersion of nanoparticles can be greatly affected by the depletion effect arising from the polymer matrix. The effect has been well investigated by the microscopic polymer reference interaction site model theory (PRISM).^{26–29} The results have shown clearly that the degree of polymerization, the detailed nature of the polymer interactions, and the spatial range of polymer matrix produce different depletion forces to nanoparticles, which greatly affect the dispersion of the nanoparticles. Compared with theory, molecular simulation provides a detailed phenomenal description. For example, Liu et al. found that polymer–filler interaction and volume fraction of polymer affect the dispersion of filler.³⁰ On the other hand, the surface modification of nanoparticles is an effective method to improve the properties of polymer nanocomposites. The grafted polymer chains on nanoparticles can also produce the similar depletion effect. It was reported that the spatial distribution of grafted fillers relates to filler size, grafting density, grafted chain length, and the matrix chain length.^{31–33} However, both of the theoretical and computational researches did not concern about the conductive mechanism of polymer nanocomposites.

In this work, we explore the conductive behavior of polymer nanocomposites based on the dispersion of nanoparticles, where the natures of nanoparticles and polymer matrix are considered simultaneously. Using the molecular dynamic simulation method, we investigate the dispersive properties affected by polymer–nanoparticle interaction strength, the grafted chains on the nanoparticles, the cross-linking of polymer chains, and blending of polymer. According to the distributions, the corresponding conductive probabilities are evaluated. Finally, the relationship between the particle dispersions and the conductive properties is discussed.

2. MODELS AND SIMULATION METHODS

In our simulations, the polymer chains are described by a bead–spring model which was developed by Kremer and Grest.³⁴ Each polymer chain consists of 30 beads with diameter equal to σ and mass equal to unity. The total number of simulated polymer beads is 12 000. Nanoparticles are modeled as Lennard-Jones (LJ) spheres of diameter D_n . Mass densities of polymer beads and the nanoparticles are the same. The truncated and shifted LJ potential for polymer–polymer, polymer–nanoparticle, and nanoparticle–nanoparticle non-bonded interactions are as follows:

$$U_{ij}(r) = \begin{cases} 4\epsilon_{ij} \left[\left(\frac{\sigma}{r - R_{EV}} \right)^{12} - \left(\frac{\sigma}{r - R_{EV}} \right)^6 \right] & 0 < r - R_{EV} < r_{cutoff} \\ -U(r_{cutoff}), & r - R_{EV} \geq r_{cutoff} \end{cases} \quad (1)$$

where r_{cutoff} expresses the distance ($r - R_{EV}$) at which the interaction is truncated and shifted to make the energy and force to be zero. We offset the interaction with a distance shifted by R_{EV} to account for the excluded volume effects of different interaction sites. For polymer–nanoparticle and nanoparticle–nanoparticle interactions, R_{EV} is $(D_n - \sigma)/2$ and $D_n - \sigma$, respectively, and for polymer–polymer interaction, R_{EV} becomes zero. The polymer–polymer interaction parameter and its cutoff distance are $\epsilon_{pp} = 1.0$ and $r_{cutoff} = 2.24\sigma$. The polymer–nanoparticle interaction strength ϵ_{pn} is changed with its cutoff distance 2.5σ .

The interaction between the adjacent bonded monomers is expressed by a stiff finite extensible nonlinear elastic potential (FENE)

$$V_{FENE} = -0.5kR_0^2 \ln \left[1 - \left(\frac{r}{R_0} \right)^2 \right] \quad (2)$$

where $k = 30e/\sigma^2$ and $R_0 = 1.5\sigma$, guaranteeing a certain stiffness of the bonds while avoiding high-frequency modes and chain crossing.

In the simulations, the NVT ensemble is employed, and the temperature is fixed at $T^* = 1.0$ by using the Nose–Hoover thermostat. Periodic boundary conditions are adopted in all three directions. The velocity-Verlet algorithm is applied to integrate the equations of motion with a time step $\delta t = 0.001$, where the time is reduced by the LJ time (τ). All structures equilibrate over a long time to make sure that all the chains have moved at least $2R_g$. The structure and dynamics data are collected for ensemble average after equilibrium. All molecular dynamic runs are carried out by using the large scale atomic/molecular massively parallel simulator (LAMMPS) developed by Sandia National Laboratories.

To determine whether the conductive network is constructed, we need a criterion to judge whether any two nanoparticles are connected. The criterion can refer to real systems. According to the field launch theory, any two carbon black fillers can be connected once their gap is less than 10 nm,³⁵ and the diameters of carbon black fillers are usually about 25–40 nm.^{36–38} In our simulation, the diameter of nanoparticles is set to 4σ or 5σ . The selected ratios of nanoparticle diameter to monomer size can in general represent polymer nanocomposites^{39–41} and are suitable for achieving relatively quick equilibria of the simulations. Compared with the real systems, the maximum gap between any two connected fillers for our model systems ranges from 1.0σ to 2.0σ . Here the uniform value 1.5σ is selected as the critical gap for conductive connection. Obviously, the value affects the absolute conductive probability but not its relative magnitude. The main purpose of the present work is to analyze the variation trends of conductivity, where the relative conductive probability is involved.

At the beginning of the computational implementation, each nanoparticle is assigned a site number and a cluster number. The site numbers are equal to the cluster numbers, ranging from 1 to N , where N is the total number of the nanoparticle. Then each nanoparticle is checked for connection with others. If two nanoparticles satisfy the connection criterion, they will be assigned a common cluster number which is the smaller one of these two nanoparticles. Finally, all the nanoparticles with the same cluster number are in the same cluster. As a result, different clusters are not connected. When nanoparticles in opposite boundary regions belong to the same cluster, the system is conducting in that direction. If there is one cluster formed in three-dimensional directions, the system transforms from nonconductivity into conductivity.

After the simulation equilibrium, more than 10 000 final configurations are dumped. At least 20 independent simulations are performed for each case to estimate the statistical error. Finally, the number of the conductive configurations is counted, and the conductive probability is thereby obtained.

3. RESULTS AND DISCUSSION

In the following discussion, we describe the dispersive states of nanoparticles through the pair correlation function, second virial coefficient B_2 , and coordination number. Here the coordination number is the average number of nanoparticles within the distance $D_n + 1.5\sigma$ around the central nanoparticle. Meanwhile, we describe the conductive properties of polymer nanocomposites by conductive probability and percolation threshold. The nanoparticle–nanoparticle pair correlation function and coordination number can be obtained directly from simulation, while B_2 can be calculated through the function ($g_{nn}(r)$)

$$B_2 = 2\pi \int_0^\infty [1 - g_{nn}(r)] r^2 dr \quad (3)$$

There are many factors to influence the dispersive and conductive behaviors. In this work, four important factors including polymer–nanoparticle interaction strength, grafted chains on the nanoparticles, cross-linking of polymer chains, and blending of polymer are concerned.

3.1. Effect of Polymer–Nanoparticle Interaction. The interaction strength between polymer and nanoparticles, representing the compatibility of polymer and nanoparticles, is the most important factor to affect the conductive properties. Here we analyze the effect of the strength to the conductivity by varying the value of ϵ_{pn} from 0.1 to 12.0. The diameter of nanoparticles is $D_n = 4\sigma$. The number of nanoparticles is 96, corresponding to a nanoparticle volume fraction of approximately $\phi_{NPs} = 18.56\%$. The selected ϕ_{NPs} should be in the percolation region. The nanoparticle–nanoparticle interaction parameter and its cutoff distance are $\epsilon_{nn} = 1.0$ and $r_{cutoff} = 1.0\sigma$, respectively. Figure 1 presents the nanoparticle–nanoparticle pair correlation function in the polymer matrix. If the interaction is relatively weak, such as $\epsilon_{pn} = 0.1$ or $\epsilon_{pn} = 1.0$, a peak appears at $r = 4\sigma$, showing a directly contact aggregation of the nanoparticles. Under low interaction strength, the depletion effect arising from the polymer chains plays the leading role, which is favorable to the aggregation of nanoparticles. If the interaction increases to 2.0, the first and the second peaks appear at $r = 5\sigma$ and $r = 6\sigma$, respectively, indicating that the depletion effect is reduced by the strong polymer–nanoparticles interactions, and the nanoparticles form aggregation sandwiched by one or two polymer layers. The

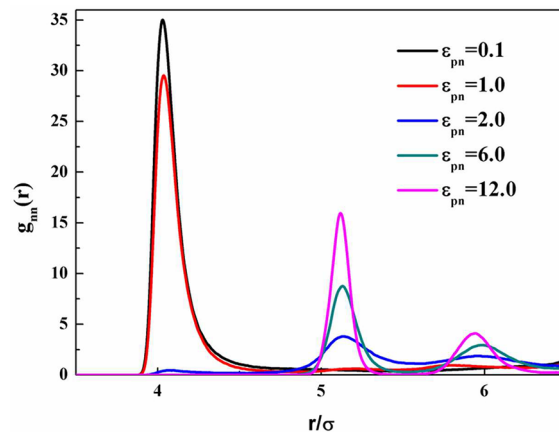


Figure 1. Nanoparticle–nanoparticle pair correlation functions with different polymer–nanoparticle interactions.

peaks at $r = 5\sigma$ and $r = 6\sigma$ become higher with the increasing interaction, meaning that more nanoparticles tend to aggregate via polymer chains.

The dispersion of particles can be further described by B_2 and the coordination number. The positive value of B_2 corresponds to stable dispersion of the nanoparticles, while the negative value means the trend to aggregation. As shown in Figure 2, the value of B_2 increases from $\epsilon_{pn} = 0.1$ to $\epsilon_{pn} = 2.0$

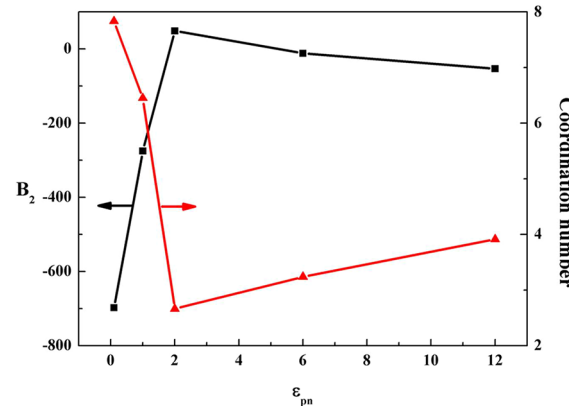


Figure 2. The left axis denotes the second virial coefficient as a function of the polymer–nanoparticle interaction, while the right axis represents the coordination number.

and decreases from $\epsilon_{pn} = 2.0$ to $\epsilon_{pn} = 12.0$. The calculated average coordination numbers are also shown in Figure 2. The minimum coordination number appears at $\epsilon_{pn} = 2.0$. The variation of the coordination number shows that, from $\epsilon_{pn} = 0.1$ to $\epsilon_{pn} = 2.0$, the nanoparticles tend to disperse, while from $\epsilon_{pn} = 2.0$ to $\epsilon_{pn} = 12.0$, they tend to aggregate. To observe the spatial distribution of nanoparticles in the polymer matrix, we change the number of nanoparticles to be 24 and get the snapshots, which are shown in Figure 3. One can see that the best dispersion occurs at $\epsilon_{pn} = 2.0$. According to Hooper and Schweizer,⁴² Figure 3 corresponds to three dispersing states: (a) microphase separation of the nanoparticles and polymer, (b) homogeneous dispersion of the nanoparticles, and (c) local bridging of the nanoparticles via the polymer chains.

Figure 4 presents the conductive probability as a function of ϵ_{pn} . Under low interaction strengths ($\epsilon_{pn} = 0.1$ and $\epsilon_{pn} = 1.0$), nanoparticles contact directly to form closed clusters, which are

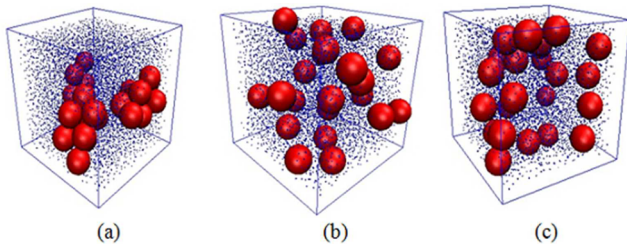


Figure 3. Snapshots corresponding to different polymer–nanoparticle interactions: (a) $\varepsilon_{pn} = 0.1$, (b) $\varepsilon_{pn} = 2.0$, and (c) $\varepsilon_{pn} = 12.0$. The red spheres denote the nanoparticles, and the polymer chains are represented by blue points for clarity.

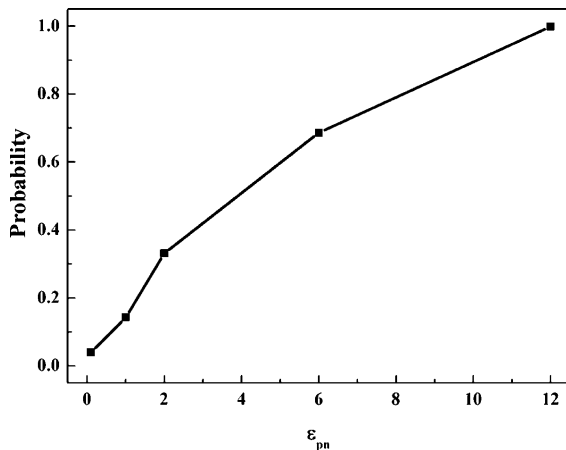


Figure 4. Conductive probability as a function of the polymer–nanoparticle interaction.

difficult to connect the opposite boundaries in three-dimensional directions, leading to a low conductive probability. As ε_{pn} increases up to 2.0, nanoparticles disperse homogeneously in the polymer matrix. Compared with those closely aggregated nanoparticles, the scattered ones have more opportunities to form a conductive network. However, since the distances between neighboring nanoparticles are too long to form a cluster, the conductivity is still low. At high interaction strengths ($\varepsilon_{pn} = 6.0$ and $\varepsilon_{pn} = 12.0$), the distances between neighboring nanoparticles are at appropriate range. It is easy to find a cluster connecting the opposite boundaries in three-dimensional directions, leading to a high conductive probability.

From Figures 2 and 4 we can find that the best dispersing state ($\varepsilon_{pn} = 2.0$) does not achieve the highest conductive probability. As ε_{pn} increases, the dispersion curve increases up to the maximum value and then decreases, whereas the conductive probability curve increases monotonously.

Conductivity of nanocomposites can be also evaluated by the percolation behavior. Figure 5 presents the conductive probabilities for polymer nanocomposites with different volume fractions of nanoparticles. For a given polymer nanocomposite (ε_{pn} is definite), if the volume fraction is relatively low, the conductive probability grows slowly with the increasing volume fraction. As the volume fraction increases to a critical value, the probability grows sharply. Then the probability grows slowly again up to the maximum value as such volume fraction is relative high. This is the typical percolation phenomenon, and the critical value is percolation threshold. Figure 5 shows clearly that the percolation threshold decreases with the increasing polymer–nanoparticle interaction. Indeed, the polymer–filler

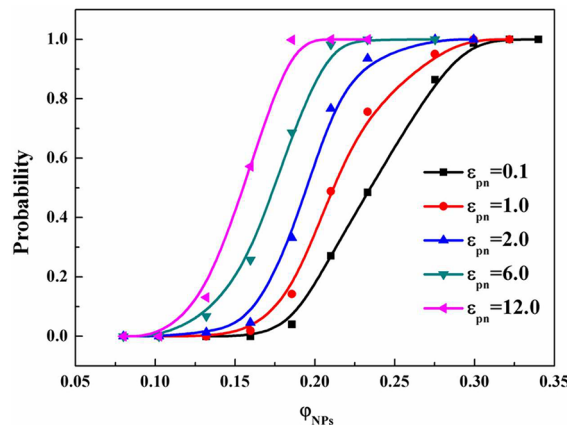


Figure 5. Conductive probability as a function of volume fraction of nanoparticles with different polymer–nanoparticle interactions.

interaction can be improved by adding chemical bonds between polymer and filler to get a low percolation threshold.⁴³

3.2. Effect of the Nanoparticle Grafted with Chains.

Surface modification of nanoparticles also obviously impacts the dispersive and conductive properties of polymer nanocomposites. The modification can be achieved by grafting polymer chains onto nanoparticles. In our simulation, each grafted chain contains 2 or 5 beads. The grafting density is expressed by the number of the chains grafted per nanoparticle (N_{gc}). The diameter of nanoparticles is set to 5σ , and the number of nanoparticles is 60. The nanoparticle–nanoparticle interaction parameter and its cutoff distance are $\varepsilon_{nn} = 1.0$ and $r_{cutoff} = 2.5\sigma$, respectively. For the grafted chain with two beads, the nanoparticle–nanoparticle pair correlation function, B_2 , and coordination numbers are calculated. Figure 6 presents the pair

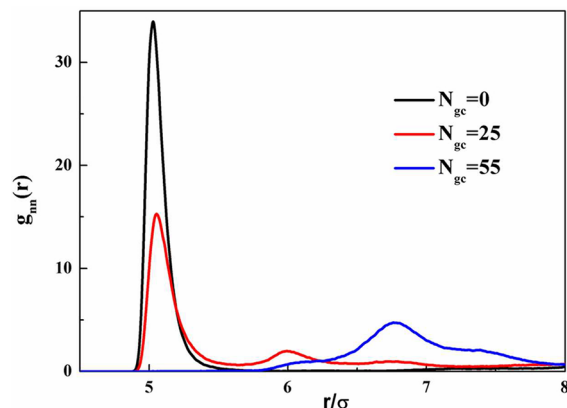


Figure 6. Nanoparticle–nanoparticle pair correlation functions for different grafting densities.

correlation function for three different grafting densities 0, 25, and 55. Figure 7 depicts B_2 and the coordination number as the function of N_{gc} . Combining the two figures, one can find that the nanoparticles tend to disperse with the increasing grafting density. In particular, in the case of high grafting density ($N_{gc} = 55$), the first peak disappears at $r = 5\sigma$, indicating that there exists no direct contact aggregation of nanoparticles and a good dispersion is thus achieved.

The corresponding conductive probabilities are then calculated and shown in Figure 8. Obviously, the curve has two peaks. The results can be explained with the schematics

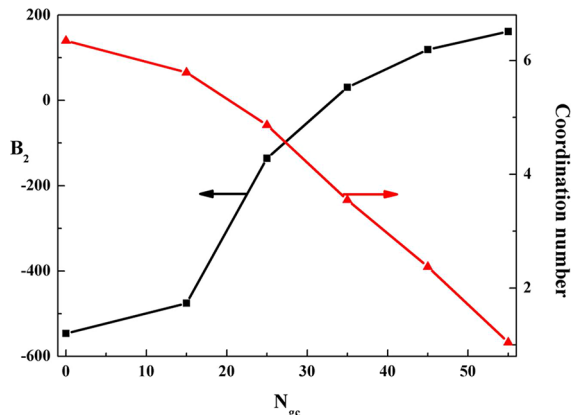


Figure 7. The left axis denotes the second virial coefficient as a function of grafting density, while the right axis represents the coordination number.

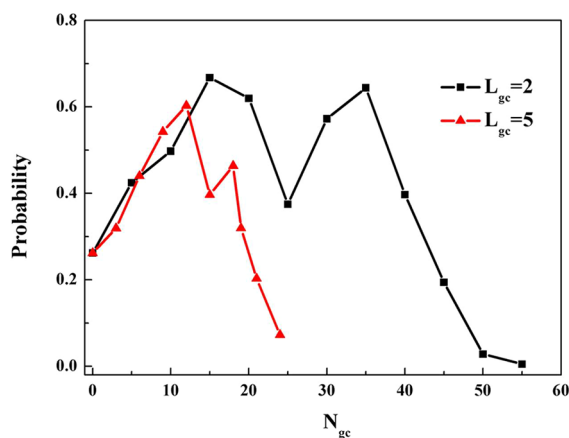


Figure 8. Conductive probability as a function of grafting density with different grafted chain lengths.

shown in Figure 9. In the nongrafting system ($N_{gc} = 0$), the surfaces of nanoparticles are not covered by grafted chains, and

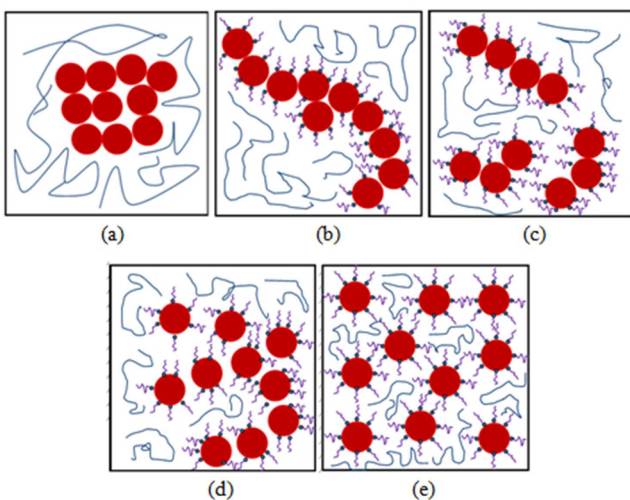


Figure 9. Schematics of the nanoparticles dispersion state corresponding to different grafting densities: (a) $N_{gc} = 0$, (b) $N_{gc} = 15$, (c) $N_{gc} = 25$, (d) $N_{gc} = 35$, and (e) $N_{gc} = 55$. The red circles denote the nanoparticles. The polymer chains and grafted chains are represented by blue and purple lines, respectively.

the nanoparticles aggregate directly to form closed quasi-spherical clusters, which causes a low conductive probability. In the low grafting system ($N_{gc} = 15$), the nanoparticle is surrounded by nanoparticles as well as grafted chains, which is favorable to form nonspherical clusters. This kind of clusters account for higher conductive probability. If the grafting density is increasing to 25, the nanoparticles are covered by more grafted chains, and the opportunity of the direct contact between adjacent nanoparticles declines. Some nanoparticles may be separated by grafted chains and form independent clusters, which declines the conductive probability. If the grafting density continues to increase to $N_{gc} = 35$, more and more nanoparticles are separated by grafted chains, forming some loose clusters. In this case, B_2 becomes positive, meaning a relatively good dispersion. The improvement of conductive probability is attributed to the good dispersion. In a high grafting density system ($N_{gc} > 35$), due to the steric effect of the grafted chains, the dispersion is very good. The nanoparticles are too far to form conductive clusters, leading to the fall of conductive probability. Especially, the conductive probability in the much higher grafting system ($N_{gc} \geq 45$) is even lower than that in the nongrafting system. To verify the results, the case of grafted chain with five beads is also simulated, and a similar conductive probability curve is obtained, which is also shown in Figure 8. Since the steric effect is more obvious for the grafted chain containing five beads, the two peaks emerge at lower grafting densities.

Combining Figures 7 and 8, we can conclude that, as the grafting density increases, the dispersion curve increases monotonously, whereas the conductive probability curve displays M-type and emerges two maximum values.

3.3. Effect of Cross-Linking of Polymer Chains. Cross-linking is an ordinary method to reinforce the mechanical properties of polymer nanocomposites. It also influences the dispersion of nanoparticles as well as the electrical conductivity of polymer matrix.⁴⁴ In real polymer nanocomposites, nanoparticles are always dispersed in a thermodynamically non-equilibrium state, and they are tend to aggregate during the usage due to the dispersion energy between nanoparticles and depletion effect of polymer matrix. In this regard, cross-linking can prevent the aggregation to some extent. In the present work, we focus on the effects of cross-linking density on the relationship between dispersion and the conductive probability. The cross-linking agents with diameter $D_{cl} = 0.5\sigma$ are added in the simulation box. The diameter of nanoparticles is $D_n = 4\sigma$. The number of nanoparticles is 96. To obtain a good dispersion of nanoparticles and cross-linking agents before the cross-linking procedure, ϵ_{pn} is set to be 2.0, and cross-linking agents are repulsive to each other. After equilibrium, chemical bonds between polymer monomer and cross-linking agent are formed if their distance is less than 0.75σ . These chemical bonds use the same FENE potential. One cross-linking agent can link two monomers, while one monomer only links one cross-linking agent. The cross-linking density is given by $\rho_{cl} = N_{cl}/M$, where N_{cl} is the number of chemical bonds formed by cross-linking and M is the number of polymer chains ($M = 400$). ρ_{cl} is changed from 0 to 10. The nanoparticles are in a dispersive state before the cross-linking. To mimic the aggregation after the cross-linking, we change the nanoparticle–nanoparticle interaction to be attractive with $\epsilon_{nn} = 6.0$ and $r_{cutoff} = 2.5\sigma$ after all the cross-linked bonds are formed.

The degree of aggregation decreases with the increasing cross-linking density, which can be verified by the increasing

value of B_2 and the decreasing coordination number, as shown in Figure 10. This is because that cross-linking significantly

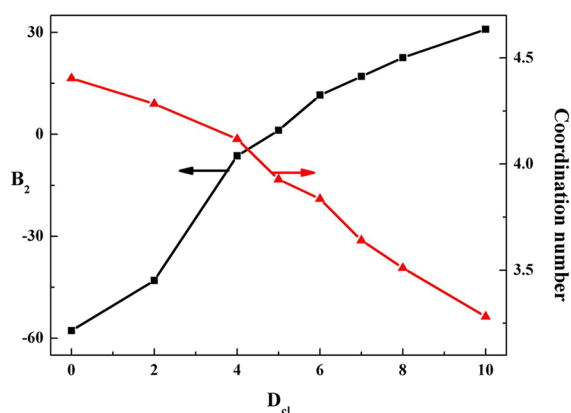


Figure 10. The left axis denotes the second virial coefficient as a function of cross-linking density, while the right axis represents the coordination number.

inhibits the aggregation of the nanoparticles. The corresponding conductive probabilities are calculated and shown in Figure 11. As cross-linking density increases, the conductive

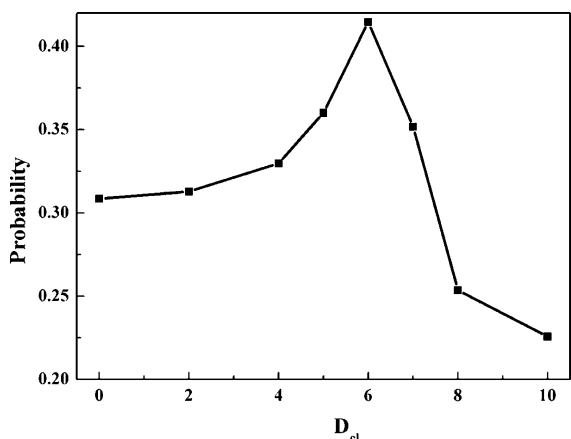


Figure 11. Conductive probability as a function of cross-linking density.

probability goes up to maximum value and then comes down. To illustrate the process, one can observe the snapshots of the distribution, which are given by Figure 12. In Figure 12a, the cross-linking density is very low, which has little influence to

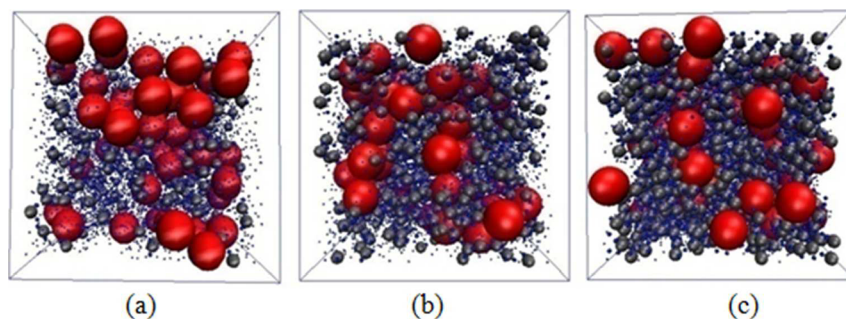


Figure 12. Snapshots corresponding to different cross-linking densities: (a) $D_{cl} = 2$, (b) $D_{cl} = 6$, and (c) $D_{cl} = 10$. The red spheres denote the nanoparticles. The polymer beads and cross-linking agent beads are respectively represented by blue points and gray spheres for clarity.

the aggregation of nanoparticles. Nanoparticles tend to form a close aggregation, leading to a bad dispersion and low probability, while in Figure 12b the cross-linking density is much larger, which has an obvious inhibition to the aggregation of nanoparticles, bringing about a relatively good dispersion and a high probability. As in Figure 12c, the cross-linking extent is high enough, nanoparticles hardly aggregate and merely form some small clusters. These clusters are separated by the dense cross-linking network. Obviously, this is harmful to the conductive behavior.

Generally speaking, the increase of the cross-linking density inhibits the aggregation of nanoparticles, and the dispersion curve increases monotonously, but the conductive probability curve increases up to a maximum and then decreases.

3.4. Effect of Selective Distribution in Polymer Blends.

Nanoparticles distributed in incompatible polymer blends also affect the percolation threshold of the polymer nanocomposite. Here we simulate nanoparticles dissolved in two incompatible polymers A and B. In the simulation box, the diameters of nanoparticles is $D_n = 4\sigma$, and polymer A and polymer B have the same chain length. The number of nanoparticles is fixed to 96, and the total number of the polymer beads keeps 12 000. The interaction strength between polymer A and nanoparticles is 2.0, while the interactions between polymer B and nanoparticles are the hard-sphere repulsion.

Figure 13 shows the calculated B_2 and the coordination number as a function of the ratio (α). Here α is the ratio of the

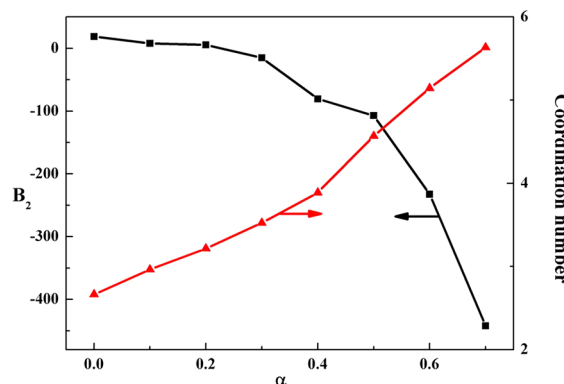


Figure 13. The left axis denotes the second virial coefficient as a function of the ratio α , while the right axis represents the coordination number.

number of polymer B beads to total number of polymer beads. As the content of polymer B increases, the dispersion of

nanoparticles becomes worse. Figure 14 is a snapshot of the dispersion. Since most of the nanoparticles exist in the phase of

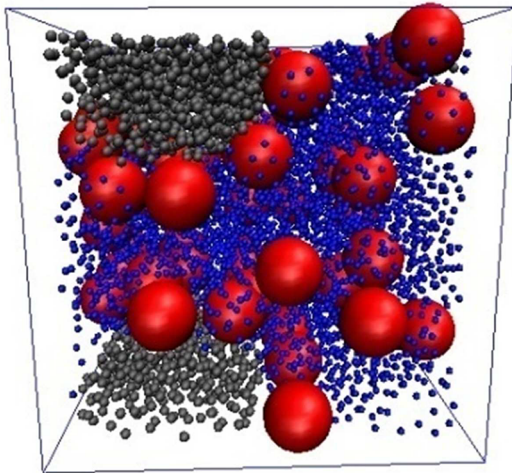


Figure 14. Snapshots corresponded to the value of α to be 30%. The red spheres denote the nanoparticles. The polymer A and polymer B chains are respectively represented by blue and gray spheres, respectively.

polymer A, increase of polymer B indicates the space for nanoparticles is gradually suppressed, and the dispersion effect monotonously declines. If the content of polymer B is less than that of polymer A, polymer A is the continuous phase, which can connect the opposite boundaries. Since the number of nanoparticles is constant, increase of polymer B means the increase of the volume fraction of the nanoparticles in the continuous phase, which facilitates the improvement of the conductive probability. If the content of polymer B is higher than that of polymer A, polymer A becomes dispersed phase. Nanoparticles in this discontinuous phase are difficult to form a contiguous conductive cluster, leading to the declines of the conductive probability. The process is illustrated in Figure 15.

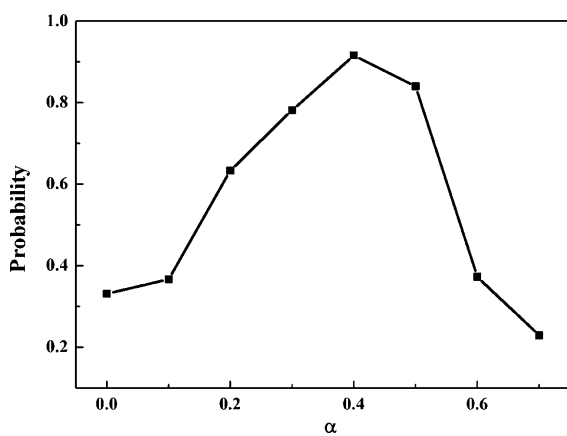


Figure 15. Conductive probability as a function of the ratio α .

We then investigate the percolation threshold by calculating the conductive probability as a function of the nanoparticles volume fraction with three different ratios of polymer B. As shown in Figure 16, polymer A is continuous phase in these cases. The percolation threshold expectantly increases with the decreasing content of polymer B.

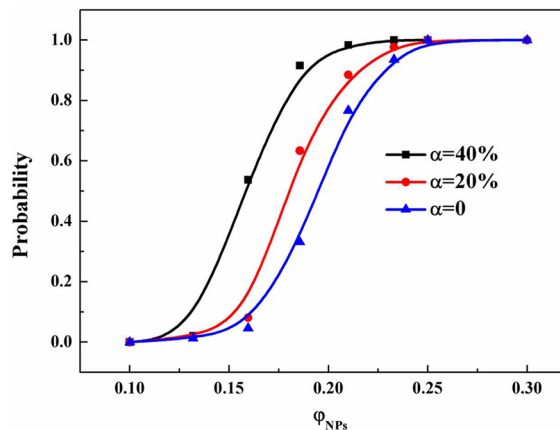


Figure 16. Conductive probability as a function of volume fraction of nanoparticles at different values of α .

The relationship between the dispersion of nanoparticles and the conductive probability of the polymer nanocomposites with above four effects is summarized in Figure 17. It is shown that

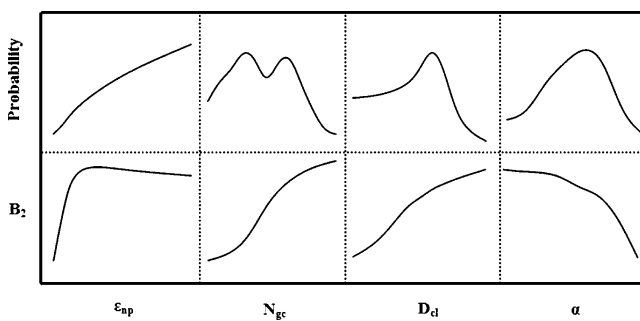


Figure 17. Probability and second virial coefficient as a function of polymer–nanoparticle interaction (ϵ_{pn}), grafting density (N_{gc}), cross-linking density (D_{cl}), and content of polymer B (α).

both dispersion and conductive probability have different changing regulations under these four different cases. All the simulations have proven that a good dispersion is not necessary for the conductive polymer composites.

4. CONCLUSION

The relationship between dispersion and conductivity of polymer nanocomposites has been studied using the molecular dynamics simulation method. By investigating four important influence factors, we find that the best dispersion does not mean the highest conductive probability. To improve the conductive properties of polymer nanocomposites, a proper increase of the dispersion of nanoparticles in polymer matrix is necessary, but an unlimited increase decreases the conductive properties. The optimum conductive probability can be obtained by increasing the grafting density, or the cross-linking density, or the incompatible polymer to an appropriate extent. Since the applied model is relatively simple, the present results merely provide a generally qualitative analysis to obtain polymer nanocomposites with relatively low nanoparticle content and good conductive properties. Further analysis is necessary in consideration of the interactions of real polymer nanocomposites.

AUTHOR INFORMATION

Corresponding Author

*E-mail: tianm@mail.buct.edu.cn (M.T.); mijg@mail.buct.edu.cn (J.M.).

Notes

The authors declare no competing financial interest.

ACKNOWLEDGMENTS

This work is supported by Program for Changjiang Scholars and Innovative Research Team in University (Grant IRT0807) and by Chemcloudcomputing of Beijing University of Chemical Technology.

REFERENCES

- (1) Fish, D.; Zhou, G.; Smid, J. *Polym. Prepr.* **1990**, *31*, 36–37.
- (2) Schaefer, D. W.; Justice, R. S. *Macromolecules* **2007**, *40*, 8501–8517.
- (3) Pang, H.; Chen, T.; Zhang, G.; Zeng, B.; Li, Z. M. *Mater. Lett.* **2010**, *64*, 2226–2229.
- (4) Bauhofer, W.; Kovacs, J. Z. *Compos. Sci. Technol.* **2009**, *69*, 1486–1498.
- (5) González-Domínguez, J. M.; Ansón-Casaos, A.; Díez-Pascual, A. M.; Ashrafi, B.; Naffakh, M.; Backman, D.; Stadler, H.; Johnston, A.; Gómez, M.; Martínez, M. T. *ACS Appl. Mater. Interfaces* **2011**, *3*, 1441–1450.
- (6) Potts, J. R.; Murali, S.; Zhu, Y. W.; Zhao, X.; Ruoff, R. S. *Macromolecules* **2011**, *44*, 6488–6495.
- (7) Jurewicz, I.; Worajittiphon, P.; King, A. A. K.; Sellin, P. J.; Keddie, J. L.; Dalton, A. B. *J. Phys. Chem. B* **2011**, *115*, 6395–6400.
- (8) Yuan, W.; Che, J. F.; Chan-Park, M. B. *Chem. Mater.* **2011**, *23*, 4149–4157.
- (9) Lyons, P. E.; De, S.; Elias, J.; Schamel, M.; Philippe, L.; Bellew, A. T.; Boland, J. J.; Coleman, J. N. *J. Phys. Chem. Lett.* **2011**, *2*, 3058–3062.
- (10) Celik, C.; Warner, S. B. *J. Appl. Polym. Sci.* **2007**, *103*, 645–652.
- (11) Fang, M.; Wang, K. G.; Lu, H. B.; Yang, Y. L.; Nutt, S. J. *Mater. Chem.* **2009**, *19*, 7098–7105.
- (12) Barman, S. N.; LeMieux, M. C.; Baek, J.; Rivera, R.; Bao, Z. A. *ACS Appl. Mater. Interfaces* **2010**, *2*, 2672–2678.
- (13) Srivastava, N. K.; Mehra, R. M. *J. Appl. Polym. Sci.* **2008**, *109*, 3991–3999.
- (14) Zou, J. F.; Yu, Z. Z.; Pan, Y. X.; Fang, X. P.; Ou, Y. C. *J. Polym. Sci., Part B: Polym. Phys.* **2002**, *40*, 954–963.
- (15) Arlen, M. J.; Wang, D.; Jacobs, J. D.; Justice, R.; Trionfi, A.; Hsu, J. W. P.; Schaffer, D.; Tan, L. S.; Vaia, R. A. *Macromolecules* **2008**, *41*, 8053–8062.
- (16) Zhang, M.; Li, D. J.; Wu, D. F.; Yan, C. H.; Lu, P.; Qiu, G. M. *J. Appl. Polym. Sci.* **2008**, *109*, 1482–1489.
- (17) Katbab, A. A.; Hrymak, A. N.; Kasparjian, K. *J. Appl. Polym. Sci.* **2008**, *107*, 3425–3433.
- (18) Kim, I. H.; Jeong, Y. G. *J. Polym. Sci., Part B: Polym. Phys.* **2010**, *48*, 850–858.
- (19) Kim, H.; Miura, Y.; Macosko, C. W. *Chem. Mater.* **2010**, *22*, 3441–3450.
- (20) Sengupta, R.; Bhattacharya, M.; Bandyopadhyay, S.; Bhowmick, A. K. *Prog. Polym. Sci.* **2011**, *36*, 638–670.
- (21) Ma, H. M.; Gao, X. L. *Polymer* **2008**, *49*, 4230–4238.
- (22) Oskouyi, A. B.; Mertiny, P. *Procedia Eng.* **2011**, *10*, 403–408.
- (23) Rahatekar, S. S.; Shaffer, M. S. P.; Elliott, J. A. *Compos. Sci. Technol.* **2010**, *70*, 356–362.
- (24) Li, C. Y.; Thostenson, E. T.; Chou, T. W. *Compos. Sci. Technol.* **2008**, *68*, 1445–1452.
- (25) Zeng, X. M.; Xu, X. f.; Shenai, P. M.; Kovalev, E.; Baudot, C.; Mathews, N.; Zhao, Y. *J. Phys. Chem. C* **2011**, *115*, 21685–21690.
- (26) Jayaraman, A.; Schweizer, K. S. *Macromolecules* **2009**, *42*, 8423–8434.
- (27) Hall, L. M.; Anderson, B. J.; Zukoski, C. F.; Schweizer, K. S. *Macromolecules* **2009**, *42*, 8435–8442.
- (28) Hall, L. M.; Schweizer, K. S. *Macromolecules* **2011**, *44*, 3149–3160.
- (29) Hall, L. M.; Schweizer, K. S. *Soft Matter* **2010**, *6*, 1015–1025.
- (30) Liu, J.; Gao, Y. Y.; Cao, D. P.; Zhang, L. Q.; Guo, Z. H. *Langmuir* **2011**, *27*, 7926–7933.
- (31) Wang, X. R.; Foltz, V. J.; Rackaitis, M.; Böhm, G. G. A. *Polymer* **2008**, *49*, 5683–5691.
- (32) Xu, C.; Ohno, K.; Ladmiral, V.; Composto, R. J. *Polymer* **2008**, *49*, 3568–3577.
- (33) Shen, J. X.; Liu, J.; Gao, Y. Y.; Cao, D. P.; Zhang, L. Q. *Langmuir* **2011**, *27*, 15213–15222.
- (34) Kremer, K.; Grest, G. S. *J. Chem. Phys.* **1990**, *92*, 5057–5086.
- (35) Van Beek, L. K.; Van Pul, B. I. *J. Appl. Polym. Sci.* **1962**, *24*, 651–655.
- (36) Cao, Q.; Song, Y. h.; qiang, T. Y.; Zheng, Q. *Carbon* **2010**, *48*, 4268–4275.
- (37) Costa, L. C.; Chakki, A.; Achour, M. E.; Graca, M. P. F. *Physica B* **2011**, *406*, 245–249.
- (38) Sisk, B. C.; Lewis, N. S. *Langmuir* **2006**, *22*, 7928–7935.
- (39) Smith, J. S.; Bedrov, D.; Smith, G. D. *Compos. Sci. Technol.* **2003**, *63*, 1599–1605.
- (40) Smith, G. D.; Bedrov, D. *Langmuir* **2009**, *25*, 11239–11243.
- (41) Hooper, J. B.; Schweizer, K. S.; Desai, T. G.; Koshy, R.; Kebinski, P. *J. Chem. Phys.* **2004**, *121*, 6986–6997.
- (42) Hooper, J. B.; Schweizer, K. S. *Macromolecules* **2005**, *38*, 8858–8869.
- (43) Deng, J. G.; Ding, X. B.; Zhang, W. C.; Peng, Y. X.; Wang, J. H.; Long, X. P.; Li, P.; Albert, S. C. C. *Eur. Polym. J.* **2002**, *38*, 2497–2501.
- (44) Abdel-Bary, E. M.; Hassan, H. H.; El-Lawindy, A. M.; Abu-Assy, M. K.; El-Tantawy, F. K. *Polym. Int.* **1993**, *30*, 371–374.